Motor Impairment in Stroke Patients Is Associated With Network Properties During Consecutive Motor Imagery

Minji Lee, Yun-Hee Kim, and Seong-Whan Lee, *Fellow, IEEE*

Abstract*—*Objective: **Our study aimed to predict the Fugl-Meyer assessment (FMA) upper limb using network properties during motor imagery using electroencephalography (EEG) signals. Methods: The subjects performed a finger tapping imagery task according to consecutive cues. We measured the weighted phase lag index (wPLI) as functional connectivity and directed transfer function (DTF) as causal connectivity in healthy controls and stroke patients. The network properties based on the wPLI and DTF were calculated. We predicted the FMA upper limb using partial least squares regression. *Results:* A higher DTF in the mu band was observed in stroke patients than in healthy controls. Notably, the difference in local properties at node F3 was negatively correlated with motor impairment in stroke patients. Finally, using significant network properties based on the wPLI and DTF, we predicted motor impairments using the FMA upper limb with a root-mean-square error of 1.68 ($R^2 = 0.97$). This outperformed the state-of-the-art predictors. *Conclusion:* These findings demonstrate that network properties based on functional and causal connectivity were highly associated with motor function in stroke patients. Significance: Our network properties can help calculate the predictor of motor impairments in stroke rehabilitation and provide insight into the neural correlates related to motor function based on EEG after reorganization induced by stroke.**

***Index Terms*—Stroke, Fugl-Meyer assessment (FMA), motor imagery, brain connectivity, network property.**

Manuscript received August 27, 2021; revised December 9, 2021 and February 9, 2022; accepted February 11, 2022. Date of publication February 16, 2022; date of current version July 19, 2022. This work was supported in part by the Institute for Information & Communications Technology Promotion (IITP) grant funded by the Korea Government under Grants 2017-0-00451, Development of BCI based Brain and Cognitive Computing Technology for Recognizing User's Intentions using Deep Learning and 2019-0-00079, Department of Artificial Intelligence, Korea University and in part by the National Research Foundation of Korea (NRF) grant funded by the Korean Government under Grant NRF-2020R1A2C3010304. *(Corresponding authors: Yun-Hee Kim; Seong-Whan Lee.)*

Minji Lee is with the Department of Brain and Cognitive Engineering, Korea University, Republic of Korea.

Yun-Hee Kim is with the Department of Physical and Rehabilitation Medicine, Center for Prevention and Rehabilitation, Heart Vascular Stroke Institute, Samsung Medical Center, Sungkyunkwan University School of Medicine, the Department of Health Science and Technology, SAIHST, Sungkyunkwan University, Seoul 06351, Republic of Korea (e-mail: yunkim@skku.edu).

Seong-Whan Lee is with the Department of Artificial Intelligence, Korea University, Seoul 02841, Republic of Korea (e-mail: sw.lee@korea.ac.kr).

This article has supplementary downloadable material available at https://doi.org/10.1109/TBME.2022.3151742, provided by the authors.

Digital Object Identifier 10.1109/TBME.2022.3151742

I. Introduction

STROKE is the primary cause of adult disability and motor impairment worldwide [1]. Stroke survivors suffer from motor and cognitive impairments, which have a significant impact on their daily lives [2]. In this regard, it is important to accurately investigate motor function to establish rehabilitation therapies in stroke patients [3]. The Fugl-Meyer assessment (FMA) [4] has been used to evaluate motor function in stroke patients. This can be used as a behavioral assessment of motor outcomes by trained experts. Thus, FMA may vary depending on the evaluator, even if appropriate training has been undertaken and standardized approaches are followed. In this respect, predicting the FMA can help reduce reliance on the proficiency and experience of such experts [5].

Motor imagery refers to the user imagining moving their affected limb as a mental rehearsal to practice actual movements [6]. Because stroke patients suffer motor impairments, motor execution can be difficult, but motor imagery can be easy. Given that motor imagery and motor execution share a neural pathway [7], brain signals during motor imagery can be utilized to predict motor function. During motor imagery, the primary motor cortex (M1), premotor area (PMA), and supplementary motor area (SMA) are activated such as motor execution in terms of motor preparation and motor planning [8]. In addition, Mizuguchi *et al.* [9] reported that the dorsolateral prefrontal cortex (DLPFC), not the sensorimotor area, is also associated with action planning. In this respect, it was found that the neural pathway of the DLPFC and SMA, and the DLPFC and PMA were shared in motor imagery and motor execution [10]. Therefore, it is necessary to include the sensorimotor area and the brain regions that serve in motor planning for predicting motor impairments.

Recently, attempts have been made to explore brain connectivity through the relationships among brain regions. Spiegler *et al.* [11] reported that functional connectivity between each side of the M1 and SMA was found in the mu band during motor imagery in healthy controls. However, no phase coupling was observed between the contralateral and ipsilateral M1 during motor imagery. In addition, Kim *et al.* [10] described the coupling strength from the PMA to the DLPFC during motor

0018-9294 © 2022 IEEE. Personal use is permitted, but republication/redistribution requires IEEE permission.
See https://www.ieee.org/publications/rights/index.html for more information.

Authorized licensed use limited to: Korea University. Downloaded on July 20,2022 at 03:25:32 UTC from IEEE Xplore. Restrictions apply.

imagery in healthy controls. Similarly, Lee *et al.* [12] reported that directional connectivity from the SMA to the DLPFC was correlated with motor imagery performance. In stroke patients, the degree of centrality in the sensorimotor area was lower than that in the initial motor imagery [13]. However, research into brain connectivity in stroke patients during motor imagery remains to be studied.

In most studies, motor imagery has been focused on a simple limb such as the left hand, right hand, or foot. However, complex motor imagery tasks, such as finger tapping, reflect corticospinal damage, which is the leading cause of permanent disability after stroke. Therefore, complex tasks are particularly relevant in assessing post-stroke motor function [14]. In addition, tapping of a finger during a sequence of trials is a good opportunity to check the motor function of the patient from the viewpoint of motor imagery learning [15]. Because reorganization of the motor network of the brain is induced through stroke [8], the brain characteristics of healthy controls and stroke patients differ during consecutive motor imagery. However, research on brain connectivity in stroke patients during these complex tasks is still needed.

In this study, we predicted motor impairments based on the FMA upper limb (UL) using electroencephalography (EEG) signals. EEG signals are widely used for identifying biomarkers because they have a high temporal resolution, and their cost is much lower than that of other neuroimaging devices [3]. We investigated the brain connectivity in healthy controls and chronic stroke patients during motor imagery. They performed consecutive finger tapping imagery tasks in repeated trials. Given that repeated trials induced motor learning, we hypothesized that later trials, as well as initial trials, during consecutive motor imagery, could be an important predictor of FMA-UL. Therefore, we analyzed both initial and later trials.

The weighted phase lag index (wPLI) and directed transfer function (DTF) were used to explore brain connectivity. Specifically, the wPLI is a functional connectivity measure to identify statistical interactions of phase lag (angles of phase locking) between two signals [16], which can be helpful for observing neural interactions between regions based on known delays for region-to-region communication [17]. In addition, DTF is a popular measure of causal connectivity for exploring the directional relationships among brain regions [18]. It is important to investigate causal relationships that consider the effects of different information flows because EEG signals are nonstationary, vary, and affect brain regions over time [19]. We also calculated the network properties based on graph theory using the wPLI and DTF. We hypothesized that the network properties would explain the brain better than the connectivity indicators themselves, given that the local and global networks work together organically [20]. Finally, we conducted correlation and regression analyses to predict motor impairments. These results can provide insight into the motor mechanism by presenting the factor associated with FMA and alleviating the difficulties faced by professionals.

The main contributions of this study can be summarized as:

- We proposed the network properties for FMA-UL using functional and causal connectivity based on the brain network.
- We compared the motor network between stroke patients and healthy controls during consecutive motor imagery in terms of motor imagery learning.
- We investigated the role of the DLPFC in directly affecting motor networks in motor impairment.

II. Related Works

EEG has long been used to predict functional outcomes, including motor impairment and motor recovery in stroke patients. Initially, the frequency, amplitude, and localization of corticoelectrical activity were proposed as biomarkers using qualitative EEG analysis [21]. However, biomarkers through this visual interpretation have low predictive performance, so quantitative EEG analysis has begun to emerge as an alternative approach. This analysis means processing EEG data with various algorithms, for example, further analyzing power ratios between specific frequency bands [21]. Finnigan *et al.* [22] reported that delta/alpha power ratio was positively correlated with patients' clinical outcomes 30 days later. Similarly, Sheorajpanday *et al.* [23] also showed that (delta + theta)/(alpha + beta) ratio had a highly positive correlation with functional outcome 6 months after ischemic stroke. In Chiarelli *et al.* [24], EEG effective power using delta, theta, alpha, and beta bands had a positive correlation with motor function, so it was used as a feature to predict recovery after 6 months. Using EEG activity during motor imagery that can provide unique information absent in resting-state, the power ratio index showed a significant negative correlation with the functional outcomes, showing the possibility of best predictor for brain-computer interface in stroke patients [25]. In fact, the power ratio index, delta/alpha ratio, and brain symmetry index in quantitative EEG analysis were used to predict FMA-UL for predicting motor recovery [26].

Brain connectivity is recently used as a reliable biomarker to characterize the brain. Tewarie *et al.* [27] showed a positive correlation between resting-state functional connectivity and oscillatory amplitude during motor execution using magnetoencephalography (MEG) signals in healthy subjects. Specifically, under global network coupling and local multi-stability, oscillatory modulation was linked with long-range connectivity. In addition, Hordacre *et al.* [28] reported that resting-state functional connectivity correlated with the response to anodal transcranial direct current stimulation (tDCS) using EEG signals in healthy subjects. Specifically, beta connectivity could be a strong predictor of tDCS effects. However, these studies did not directly investigate the relationship between motor function outcomes and participation in stroke patients.

Neurophysiological biomarkers based on brain connectivity were used to predict motor impairment or motor recovery. Rathee *et al.* [29] reported the prediction of post-stroke UL using a resting-state functional network based on MEG signals. The inter-hemispherical network was positively correlated with motor cortical regions. However, this work is less practical when using MEG signals. Philips *et al.* [30] used functional connectivity in EEG signals during the movement of the shoulder and elbow. They reported a negative correlation between the density of the unaffected hemisphere and the FMA-UL score for motor recovery using Spearman's correlation ($rho = -0.46$). High

Authorized licensed use limited to: Korea University. Downloaded on July 20,2022 at 03:25:32 UTC from IEEE Xplore. Restrictions apply.

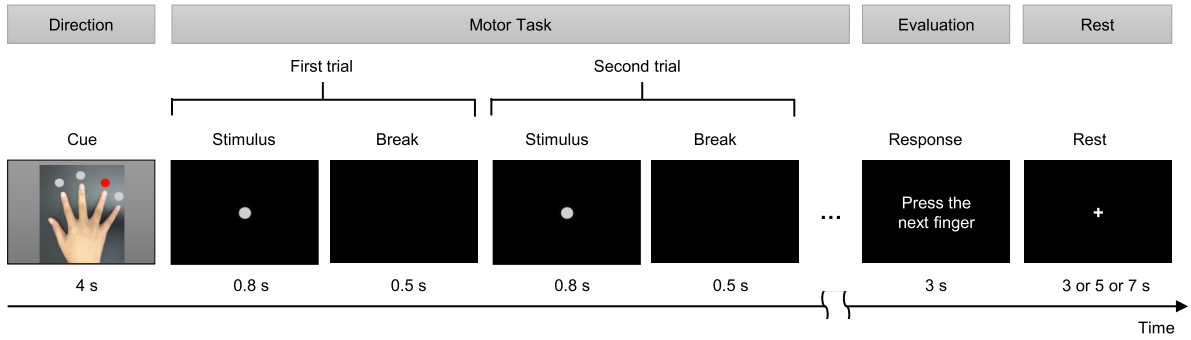

Fig. 1. Experimental design in one block. The first finger to tap is presented as a red dot, and the fingers are then imagined at 1.3 s intervals for each dot in the given order. At least three white dots are indicated. At the end of the block, as the evaluation part, the subjects actually press their fingers in turn.

initial values of local efficiency over the beta band also predicted motor improvements based on the FMA-UL ($R^2 = 0.16$). Riahi *et al.* [5] estimated the FMA-UL using functional connectivity. Specifically, alpha coherence showed a positive correlation with FMA-UL. The authors predicted FMA-UL using partial least squares regression and resulted in an R^2 of 0.91 in all ten stroke patients.

However, related studies did not use directed connectivity, such as causality, and measured functional connectivity, which does not reflect the time-series information. In addition, motor function in stroke patients was evaluated based on functional connectivity, but no comparison was explored for healthy subjects with normal motor function. Therefore, it is unclear which are reliable biomarkers. In this study, we further calculated the causal connectivity to explore the direction of brain connectivity. In addition, the brain connectivity in healthy subjects was compared. The proposed network properties would complement motor assessments for predicting the FMA-UL.

III. Materials and Methods

A. Subjects

Twelve healthy controls (54.8 ± 2.2; F = 4) and twelve chronic stroke patients (53.8 ± 6.5; F = 5) were enrolled in this study. The data were previously published by Lee *et al.* [15]. Supplementary Table I shows the clinical information of the chronic stroke patients. Please see the Supplementary Document for detailed inclusion and exclusion criteria. This study was approved by the Institutional Review Board (IRB) at Samsung Medical Center (SMC 2013-02-091) and written informed consent was obtained from all subjects.

B. Experimental Paradigm

A sequential finger tapping imagery task was conducted using the affected hand in stroke patients. In healthy controls, during motor imagery with both hands separately or both hands together, dominant M1 was activated whereas non-dominant M1 was deactivated [31]. In other words, the corticomotor excitability of dominant M1 increased regardless of the moving direction of the hand. In this regard, the dominant hand was used in healthy controls to maximize the network difference compared to the lesion side of stroke patients [15]. All controls were right-handed using the Edinburgh Handedness inventory [32].

Our experimental design was a trial-randomized block design. This paradigm was composed of 20 blocks, and each block consisted of direction, motor imagery task, evaluation, and resting parts. There were at least three trials for each block. This was done to prevent habitual pressing during the evaluation of each block. Fig. 1 represents the experimental design of a block. For the direction part, an image of the hand was marked by a specific finger with a red dot to indicate the tapping of the starting finger during the motor imagery task. The finger used to start the tapping task was randomly presented in each block. An image was shown for 4 s. In the motor task part, at least three or more stimuli were given a white dot every 1.3 s. The subjects were instructed to imagine tapping the button whenever a white dot appeared. The white dot was presented for 0.8 s and then disappeared. The number of dots was random to avoid the prediction of the final tapping finger during the evaluation part. A black screen was then shown for 0.5 s. The order of finger tapping was from the index finger to the little finger except for the thumb. After the little finger was over, it was the order of the index finger again. At the end of the experiment, an evaluation was conducted. The subjects were instructed to press the next finger to be tapped physically. For example, if the index finger was marked with a red dot in the direction, it was followed by three white dots. Then, in the motor task part, the subject imagined tapping their index finger, middle finger, and ring finger in order. During the evaluation, it was considered that pressing the little finger resulted in the correct block of the motor imagery. If the subject pressed the other finger, not the little finger, this can be clearly judged that the subject did not properly imagine. In this regard, we considered an accurate performance as corresponding to the actual conduction of a motor imagery task. Finally, a rest period was provided with a plus sign, which was randomly presented for 3, 5, or 7 s to minimize the impact on the next block.

C. EEG Acquisition and Pre-Processing

The EEG signals were measured using a Neuro-Prax EEG system (NeuroConn GmbH, Germany) from 27 surface Ag/AgCl

Authorized licensed use limited to: Korea University. Downloaded on July 20,2022 at 03:25:32 UTC from IEEE Xplore. Restrictions apply.

electrodes (Easy Cap, Germany) using the international 10–10 system. Signals were collected from a sample rate frequency of 4,000 Hz.

The data were processed using the EEGLAB toolbox [33] with MATLAB R2018b (MathWorks, USA). The EEG data were down-sampled at a rate of 500 Hz. Continuous signals were filtered from 1 to 45 Hz using a basic finite impulse response (FIR) filter. Artifacts such as eye blinks were removed from the data using independent component analysis, which were then segmented into −1.5–4 s epochs based on the dot during the first trial. EEG data were re-referenced to the average of all electrode potentials [34]. In this way, because there were at least three trials for each block conducted every 1.3 s, we measured the epoched data for the three trials of each block. A pre-stimulus baseline of the epoched data during the −1.5–0 s period was removed. Finally, since there were at least three trials in one block, we included only the (initial) first and (later) third trials.

The EEG data were filtered into two frequency bands (mu band of 8–12 Hz and a beta band of 13–30 Hz) related directly to the motor function using an FIR filter. As a result of the evaluation part, the epoched EEG data from the incorrect responses were excluded from further analysis. Thus, an average of 17.67 ± 2.23 and 13.50 ± 5.84 blocks out of 20 blocks was used for healthy controls and stroke patients, respectively. Furthermore, since healthy controls conducted motor tasks using their right hand (dominant hand), the EEG signals in 5 of the 12 chronic patients who suffered the stroke in the right hemisphere were mirrored across the midline for homogeneity and statistical analysis.

D. Connectivity Estimator

The brain network consists of a node and an edge connecting these nodes. Here, the channel is considered as a node. Supplementary Fig. 1 shows the overall flowchart for measuring the connectivity estimators and network properties.

1) Functional Connectivity: We used the wPLI as a connectivity measure between the two nodes. This allowed phase lag interactions to be detected from a complex coupled brain network. In addition, this method is robust to volume conduction and noise artifacts [16]. We calculated 27 × 27 wPLI between the two nodes in all brain regions as follows.

$$wPLI = \frac{|E\{\mathcal{J}\{X\}\}|}{E\{|\mathcal{J}\{X\}|\}} = \frac{|E\{|\mathcal{J}\{X\}|sgn(\mathcal{J}\{X\})\}|}{E\{|\mathcal{J}\{X\}|\}} \quad (1)$$

where $\mathcal{J}\{X\}$ means the imaginary component of the cross-spectrum $X = Z_i Z_j^*$ between two nodes i and j, Z_i and Z_j^* indicate the complex-valued Fourier transform of the signal of node i and the complex conjugate of Z_j, respectively. In addition, $E\{\bullet\}$ refers to the expected-value operator.

2) Effective Connectivity: The DTF for the causal relationship between two nodes was calculated using the HERMES toolbox [35]. This uses a multivariate autoregressive model and is robust to volume conduction effects [18].

$$DTF_{ij}(f) = \frac{H_{ij}(f)}{\sqrt{h_j^H(f)h_j(f)}} \quad (2)$$

where $DTF_{ij}(f)$ indicates DTF from node i to node j. i means the row of the $H(f)$ matrix and j and m are its columns. $H(f)$ refers to the transfer function matrix: $H(f) = [I - A(f)]^{-1}$, where $A(f)$ is the Fourier transform of the coefficients. Moreover, $(.)^H$ indicates the Hermitian transpose [35].

The DTF was normalized to the total outflow of information [35]. In other words, row-wise normalization limits incoming connection values to regions. Thus, the value of each incoming connection strength is decided together by the other connection strengths. This means that increasing the impact strength from one region to the target region reduces the connection value to another region [36]. Therefore, DTF can affect indirect connections. In this regard, DTF does not distinguish between direct and indirect interactions.

3) Thresholding Connectivity Measure: We then applied the threshold for subject-wise matrices. This is important to decrease the possibility of false negatives, while only identifying functionally relevant connections [37]. To explore the optimal connection density, we used the mean global and local efficiencies from 100 random graphs with 27 nodes. Here, global efficiency refers to the aggregated capacity of integrated processing, whereas local efficiency refers to the local information of segregated processing in the brain network [20]. The threshold density was selected when the differences between the global and local efficiencies were maximized (density = 0.302) [38]. Therefore, among all 729 connections in the 27 × 27 wPLI in the brain network, only 210 strong connections remained.

E. Network Properties

Network analysis can characterize brain connectivity as a small number of neurobiologically easily and useful calculated measurements. These properties detect various functional integration and separation of the brain and quantify the centrality of individual brain regions or pathways [20]. Based on the connectivity measures, we calculated the global and local properties using the Brain Connectivity Toolbox [20]. These were calculated in the mu and beta bands, and local properties were measured over five regions (DLPFC, PMA, SMA, contralateral M1, and ipsilateral M1) related to a motor network [9]. Specifically, we considered node C3 as contralateral (ipsilesional) M1, node C4 as ipsilateral (contralesional) M1, node Cz as SMA, node Fz as PMA, and node F3 as the left DLPFC [39], [40].

1) Global Efficiency: The global efficiency (E_{glob}) represents the mean inverse of the shortest path length in all pairs of nodes as a measure of integration.

$$E_{glob} = \frac{1}{N}\sum_{i\in N}\frac{\sum_{j\in N, i\in j} d_{ij}^{-1}}{n-1} \quad (3)$$

where d_{ij} indicates the shortest path length between nodes i and j, and N and n refer to the number of all nodes in the network and the number of individual nodes, respectively [20]. Global efficiency is primarily influenced by short paths; therefore this can be a better measure of network integration compared to the average shortest path length [41].

2) Local Efficiency: The local efficiency (E_{loc}), as a measure of segregation, represents the mean of all global efficiency

Authorized licensed use limited to: Korea University. Downloaded on July 20,2022 at 03:25:32 UTC from IEEE Xplore. Restrictions apply.

in every sub-network on each node [20].

$$E_{loc} = \frac{1}{N}\sum_{i \in N} E_{glob}(A_i) \tag{4}$$

where A_i is the sub-network of the first neighbours of node i [42].

3) Eigenvector Centrality: Eigenvector centrality is a self-referential measure of centrality and has a higher value associated with many other nodes [20]. In addition, this detects the nodes connected to high-degree nodes that have many connections with other neighboring nodes as the measure of centrality in the network [43]. This measure is computed as the spectral measure of centrality:

$$Ax = \lambda x \tag{5}$$

where matrix A is the weighted matrix of wPLI. λ is the largest eigenvalue and x is the corresponding eigenvector.

$$x_i = \mu \sum_{n=1}^{N} a_{ij} x_j \tag{6}$$

where $\mu = 1/\lambda$ such that x_i represents the eigenvector centrality of node i in the normalized eigenvector belonging to the largest eigenvalue of A in the brain network [44].

4) Degree: The degree in node i (D_i) is calculated as the number of links connected to a node.

$$D_i = \sum_{j \in N} W_{ij} \tag{7}$$

where W_{ij} refers to the connection weights between nodes i and j when nodes i and j are neighbors [20].

In directed connectivity, it can be extended to in-degree and out-degree in each node.

$$D_i^{\text{in}} = \sum_{j \in N} a_{ji} \tag{8}$$

$$D_i^{\text{out}} = \sum_{j \in N} a_{ij} \tag{9}$$

where a_{ij} refers to the connection weights from node i to node j. In other words, a_{ij} is not always equal to a_{ji} [20].

F. Evaluation

The averaged connectivity measures and network properties across all blocks for each subject were used to predict the FMA-UL. Pearson's correlation analysis was calculated. In detail, correlation between each connectivity measure and FMA-UL scores was computed for all stroke patients. We also used the global permutation test to evaluate the significance of the correlation coefficient with multiple comparisons [5]. This test evaluates whether the effect expressed as a latent variable, a given unobservable variable, is strong enough to differ from random noise in a statistical sense [45]. The response variable (FMA-UL scores of the patients) was randomly shuffled at 1,000 times while keeping the original order of the predictor variable (connectivity features). This means that a new singular value sample is obtained by reordering the FMA-UL scores. Then, the distribution of singular values obtained from the randomization test was generated. If a singular value is within the top 50 samples of the distribution under the null hypothesis, it is considered statistically significant.

To predict the FMA-UL in patients, we carried out partial least squares regression [46] using connectivity measures and their network properties. This is well suited for analyzing electrophysiological activities using a multivariate statistical approach [45]. A leave-one-out approach was used for training and testing [5]. For the performance measure, the root-mean-square error (RMSE), and R^2 were applied during the regression analysis. The RMSE indicates the difference between the actual and predicted FMA-UL, and R^2 represents how close the predicted data are to the fitted regression line [47].

In addition, we compared the predictive performance with state-of-the-art methods. The brief descriptions of each method are as follows.

- Wu *et al.* [46] computed coherence as functional connectivity in high beta band (20–30 Hz). Next, they used the coherence between the ipsilesional M1 (C3) and PMA (Fz) for predicting FMA-UL.
- Philips *et al.* [30] used the generalized measure of association (GMA) as functional connectivity in the beta band (12.5–25 Hz). The connectivity measure was then applied to a threshold of 0.05. Finally, the local efficiency was computed for all nodes.
- Riahi *et al.* [5] used the phase lag index (PLI) for nodes FP2-F7, F7-F3, F8-C4, and FC2-Cz at a medium alpha frequency (11 Hz). This predictor was the highest compared to other connectivity measures (spectral coherence, imaginary part of coherence, phase clustering, and wPLI).

G. Statistical Analysis

We compared the behavioral accuracy of motor imagery tasks between healthy controls and patients that had a stroke. Non-parametric permutation-based t-tests were used with Bonferroni correction for multiple comparisons. To compare the difference in the wPLI, DTF, and network properties between healthy controls and stroke patients, the non-parametric permutation-based t-tests were also performed ($r = 1{,}000$). In addition, the non-parametric permutation-based t-tests with Bonferroni correction for multiple comparisons were used to investigate the changes in network properties from the first trial to the third trial within groups. These permutation tests are very effective for statistical analysis of non-parametric data by using surrogate data for sufficient sets of statistics in the null hypothesis [48]. The significance level was considered to be a p-value of 0.05.

IV. Results

A. Behavioral Difference of Motor Imagery Between Groups

The subjects were first told to imagine using their fingers to tap buttons. Then, we evaluated whether they clearly performed the motor imagery through the final fingers that had to be pressed at the end. This behavioral accuracy decreased when

Authorized licensed use limited to: Korea University. Downloaded on July 20,2022 at 03:25:32 UTC from IEEE Xplore. Restrictions apply.

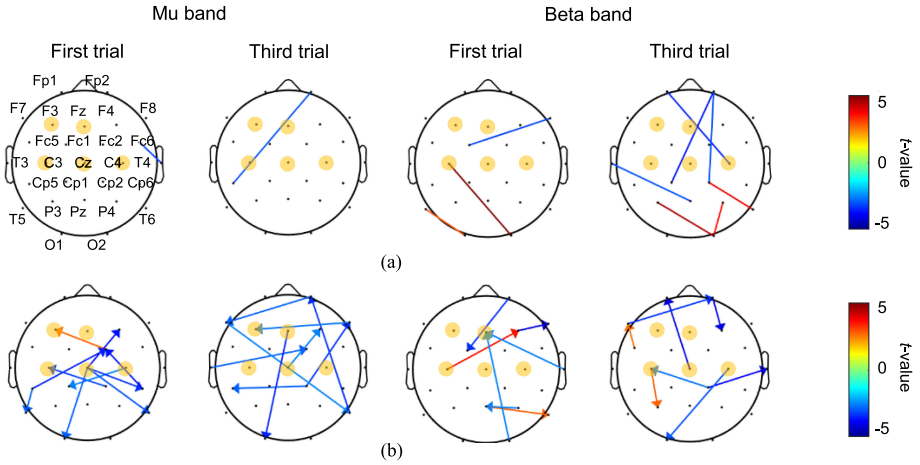

Fig. 2. Topological differences in connectivity measures between healthy controls and stroke patients. This represents the averaged results of all stroke patients and healthy controls in (a) wPLI and (b) DTF. The position of each channel represents the node, and the edge connecting the node is represented by the t-value using a non-parametric permutation test with Bonferroni correction for the connectivity measures between healthy controls and stroke patients. Here, we only drew edges with significant differences that had a p-value of less than 0.05 with Bonferroni correction to show a significant difference. We highlighted five nodes (node C3 as the contralateral (ipsilesional) M1, node C4 as the ipsilateral (contralesional) M1, node Cz as the SMA, node Fz as the PMA, and node F3 as the left DLPFC) of interest in yellow. The red line indicates statistically stronger connections of healthy controls, and the blue line indicates a statistically stronger connection of stroke patients. The left hemisphere indicates the contralateral or ipsilesional direction in healthy controls and stroke patients, respectively. In other words, in these plots, all subjects performed the finger tapping task with their right hands.

the subject pressed the wrong finger or failed to press the finger. The accuracy of behavior in consecutive motor imagery provided information on whether motor imagery had actually been clearly performed, which was also related to clear EEG patterns during motor imagery. In imagery tasks, it was usually unclear whether the subject actually performed their imagined movement or remained still. The results showed that the behavioral accuracy in healthy controls and stroke patients was $88.33 \pm 11.15\%$ (mean $\pm$ standard deviation) and $67.50 \pm 29.19\%$ using the dominant or affected hand, respectively. The performance in stroke patients was significantly lower than in healthy controls ($t = -2.304$, $p = 0.039$). We excluded the incorrect block from further analysis.

B. Difference in Brain Connectivity Between Groups

1) Functional Connectivity: Fig. 2(a) shows the differences in the wPLI between stroke patients and healthy controls over the mu and beta bands. The front-parietal connection was generally prominent, especially in stroke patients. In beta band, the wPLI in healthy controls was stronger compared to stroke patients, especially in parietal region.

However, there were no differences in 20 connections of the motor network including the DLPFC between healthy controls and stroke patients in both trials and frequency bands.

2) Effective Connectivity: We observed a higher DTF in stroke patients over the mu band compared to healthy controls in both the first and third trials (Fig. 2(b)). Specifically, long connectivity between the front and back was observed, rather than connections between the two hemispheres.

In addition, we compared the motor network of the DTF between stroke patients and healthy controls. In particular, there was a statistically significant difference in DTF from Cz to other nodes (Supplementary Fig. 2). In the first trial, DTF from Cz to Fz ($t = -2.456$, $p = 0.021$) and C3 ($t = -2.359$, $p = 0.031$) in stroke patients was higher than in healthy controls over mu band. On the other hand, in the third trial, there was a higher DTF from Cz to C4 ($t = -2.608$, $p = 0.029$) in the mu band. The outliers shown in Supplementary Fig. 2 were all different subjects, which did not have a high DTF of a particular subject. Moreover, there was a higher DTF from Cz to F3 ($t = -1.979$, $p = 0.045$) over the beta band in stroke patients than in healthy controls. In addition, a higher DTF from C4 to F3 was found in stroke patients than in healthy controls ($t = -2.717$, $p = 0.029$) in the beta band.

C. Difference in Network Properties Within Groups

Based on these results, we compared the network properties of each group for repeated trials during consecutive motor imagery. In the global efficiency based on the wPLI and DTF, there were no significant differences between the first and third trials over both the mu and beta bands in stroke patients. Likewise, there was no change in consecutive trials in the healthy controls.

Fig. 3 shows the local properties based on the wPLI in node F3 over the mu band. In healthy controls, there were no significant differences in the degree, local efficiency, and eigenvector centrality between the first and third trials. However, in stroke patients, those in the first trial were significantly higher than those in the third trial at node F3 (degree: $t = 3.835$, $p = 0.003$; local efficiency: $t = 3.500$, $p = 0.007$; eigenvector centrality: $t = 4.570$, $p < 0.001$). In specific, healthy controls showed changes in degree from 8.16 ± 2.69 to 8.66 ± 5.05, whereas stroke patients showed changes in degree from 9.16 ± 4.26 to 5.50 ± 2.71. Next, in local efficiency, it changed from 0.72 ± 0.10 to 0.63 ± 0.16 in healthy controls, and from 0.73 ± 0.15 to 0.53 ± 0.28 in stroke patients, respectively. In eigenvector centrality,

Authorized licensed use limited to: Korea University. Downloaded on July 20,2022 at 03:25:32 UTC from IEEE Xplore. Restrictions apply.

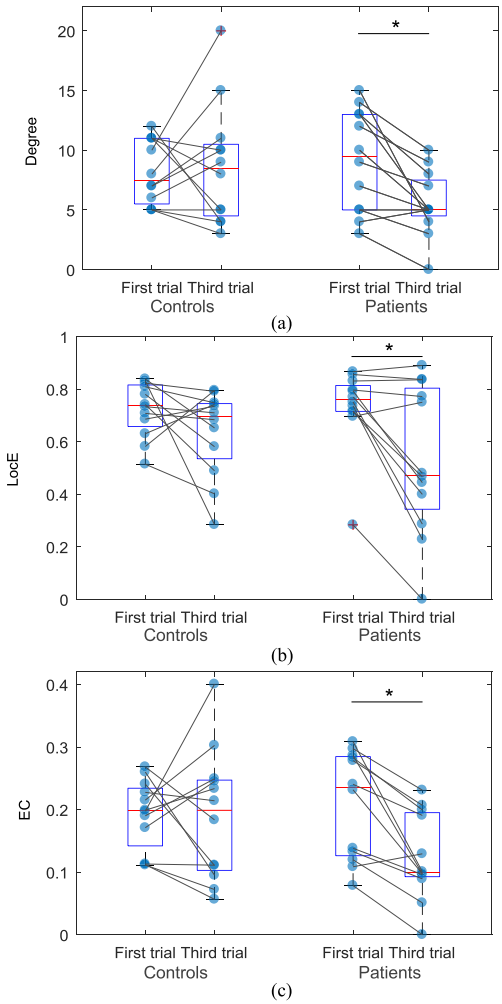

Fig. 3. Difference in mu network properties at node F3 between healthy controls and stroke patients. We investigated (a) degree, (b) local efficiency, and (c) eigenvector centrality over mu band based on the wPLI. Each point is the averaged local properties on the blocks in each subject. The error bars indicate the standard deviation. * indicates significance using non-parametric permutation-based t-tests between trials ($p < 0.05$) with Bonferroni correction.

changes from 0.19 ± 0.05 to 0.18 ± 0.10 in healthy controls and from 0.20 ± 0.08 to 0.12 ± 0.06 in stroke patients were observed. In the beta band, there was a significant difference in only local efficiency based on the wPLI in stroke patients at node Fz ($t = 1.478$, $p < 0.001$).

In DTF-based local properties, only local efficiency in stroke patients over the mu band was observed ($t = 1.942$, $p = 0.031$). No significant differences in eigenvector centrality, in-degree, and out-degree were observed in both healthy controls and stroke patients.

D. Correlation With FMA-UL in Stroke Patients

1) Connectivity Measure: We explored the correlation with FMA-UL in the motor network of the wPLI and DTF in stroke patients. A positive correlation with FMA-UL was observed only for the wPLI between nodes C3 and C4 ($rho = 0.723$, p-value $= 0.007$). Except for that, there was no relationship between the wPLI in 19 connections of the motor network with FMA-UL.

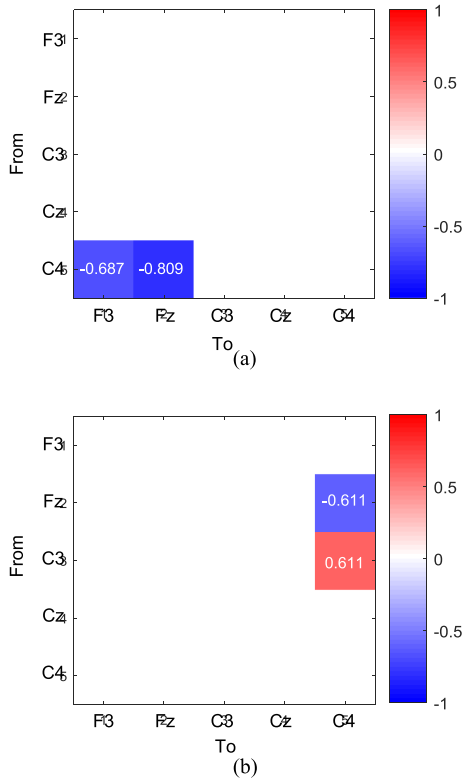

Fig. 4. Correlation between DTF and FMA-UL in stroke patients. The correlation coefficient with directional connectivity was calculated using (a) mu band with the third trial and (b) beta band with the first trial.

We also found a statistical correlation between DTF in the motor network and the FMA-UL. In the mu band with the first trial, there was no correlation with FMA-UL. In the third trial over the mu band, we showed the DTF from C4 to F3 and Fz negatively correlate (Fig. 4(a)). In the beta band, DTF from Fz to C4 was negatively correlated with FMA-UL, whereas DTF from C3 to C4 was positively correlated (Fig. 4(b)). Finally, no relationship was observed in the third trial over the beta band.

2) Network Properties: As a global property, we measured the global efficiency, and as the local properties, we calculated the local efficiency, eigenvector centrality, and degree based on the wPLI and DTF. Fig. 5 shows the relationship between global efficiency using the wPLI and FMA-UL. Only the wPLI-based global efficiency in the first trial over the beta band was positively correlated with the FMA-UL ($rho = 0.680$, $p = 0.015$). On the other hand, when the third trial was used, there was no significant relationship with FMA-UL.

We explored the local properties of each five node. At node F3, there was a negative correlation with the wPLI-based local efficiency in the first trial over the beta band ($rho = -0.643$, $p = 0.023$). We found the statistical relationship at node Fz (Fig. 6). There was a positive correlation between FMA-UL and wPLI-based local efficiency in the first trial ($rho = 0.668$, $p = 0.018$). In the third trial over mu band, wPLI-based degree and

Authorized licensed use limited to: Korea University. Downloaded on July 20,2022 at 03:25:32 UTC from IEEE Xplore. Restrictions apply.

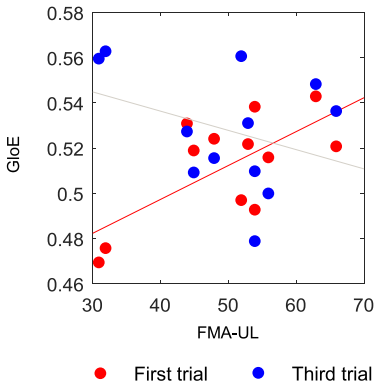

Fig. 5. Correlation with global efficiency based on wPLI over beta band. The red and blue dots indicate the global efficiency in the first and third trials, respectively. Each dot means averaged global efficiency of the corresponding trial in all blocks on each subject. The solid lines represent linear fits to the data. In particular, the gray line refers to no significant correlations with a p-value of 0.05 or less, and the red or blue line indicates that each global efficiency (GloE) is statistically correlated with the FMA-UL.

TABLE I
PREDICTION OF FMA-UL USING LEAVE-ONE-OUT CROSS-VALIDATION

Patient	Actual FMA-UL	Predicted FMA-UL				
		wPLI	DTF	wPLI-NP	DTF-NP	All NP
P01	32	35.91	30.07	32.35	41.35	30.70
P02	44	48.78	40.76	46.95	50.68	44.52
P03	31	33.61	37.14	32.80	36.28	32.26
P04	56	51.19	55.94	53.23	52.77	55.46
P05	52	60.22	59.42	54.97	47.22	54.89
P06	54	54.06	56.68	45.82	49.31	51.51
P07	53	51.82	51.17	51.31	57.86	54.67
P08	54	56.17	54.71	57.87	43.57	55.11
P09	45	53.35	44.74	48.55	54.65	46.48
P10	48	51.26	54.18	51.49	41.37	45.37
P11	63	48.45	56.09	55.53	62.21	62.45
P12	66	53.17	57.09	67.12	60.73	64.57
RMSE		7.06	4.86	4.03	6.54	*1.68*
R^2		0.52	0.77	0.84	0.59	*0.97*

NP = network properties.

eigenvector centrality were negatively correlated with FMA-UL (degree: $rho = -0.749$, $p = 0.005$; eigenvector centrality: $rho = -0.726$, $p = 0.008$). At node C3, there was no correlation with the local properties. In the first trial, there was a negative correlation in the wPLI-based degree in the node Cz ($rho =$ -0.620, $p = 0.031$) and DTF-based local efficiency in node C4 ($rho = -0.714$, $p = 0.009$).

E. Prediction of Motor Impairment in Stroke Patients

We predicted the FMA-UL using connectivity measures and network properties were statistically correlated with the FMA-UL in stroke patients. We also used leave-one-out cross-validation based on the partial least squares regression. Table I shows the predicted FMA-UL using wPLI, DTF, and their network properties using partial least squares regression.

TABLE II
COMPARISON OF PROPOSED METHOD WITH STATE-OF-THE-ART STUDIES

Method	Use of trial	RMSE	R^2
Wu *et al.* [46]	First + third trials	9.04	0.22
Philips *et al.* [30]	First trial	9.95	0.05
Riahi *et al.* [5]	First + third trials	5.78	0.68
Proposed Method *(Ours)*	First + third trials	*1.68*	*0.97*

In the wPLI, we predicted only one feature (beta wPLI between C3-C4 with the third trial) that was correlated with FMA-UL. Using the DTF, as shown in Fig. 5, four features (mu DTF from C4 to F3 and Fz, beta DTF from Fz and C3 to C4) were used to predict FMA-UL. Compared with the connectivity indicators, the RMSE was low, and R^2 was high when DTF was used. In other words, performance using causal connectivity was the highest. In the wPLI-based network properties, six features (beta global efficiency with the first trial, mu local efficiency with the first trial, mu degree and eigenvector centrality with the third trial, beta degree and local efficiency with the first trial) were used, whereas two features (beta local efficiency with the first trial over node Fz and C4) in the DTF-based network properties were used. Finally, the prediction was best when all network properties based on the wPLI and DTF correlated with FMA-UL were used.

F. Comparison of Our Method With State-of-The-Art Studies

We computed the predictive performance of the FMA-UL using the state-of-the-art studies shown in Table II. In Wu *et al.* [46] used high beta coherence between nodes C3 and Fz. Using only the first trials, the RMSE and R^2 were 9.773 and 0.087, respectively. In the third trial, the performance was slightly improved, with RMSE and R^2 values of 9.279 and 0.177, respectively. However, when combined with the first and third trials, RMSE and R^2 had the highest performances of 9.042 and 0.218, respectively.

Philips *et al.* [30] used the local efficiency based on the GMA. When the first and third trials were used, the RMSEs were 9.950 and 10.183, and R^2 was 0.054 and 0.009, respectively. However, the combination of the first and third trials resulted in a lower performance than the first trials, with RMSE and R^2 values of 9.892 and 0.065, respectively.

Riahi *et al.* [5] computed the PLI over a medium alpha frequency. In the first trial, the RMSE and R^2 were 8.409 and 0.324, respectively. In addition, RMSE and R^2 were 7.221 and 0.502, respectively, when only the PLI with the third trial was used. When both trials were used, the RMSE and R^2 were 5.780 and 0.681, respectively, and the performance was higher than when each trial was used.

Except for local efficiency, the predictive performance was higher in both the coherence and PLI trials. Nevertheless, the proposed model showed a higher predictive performance than the best from each state-of-the-art method.

Authorized licensed use limited to: Korea University. Downloaded on July 20,2022 at 03:25:32 UTC from IEEE Xplore. Restrictions apply.

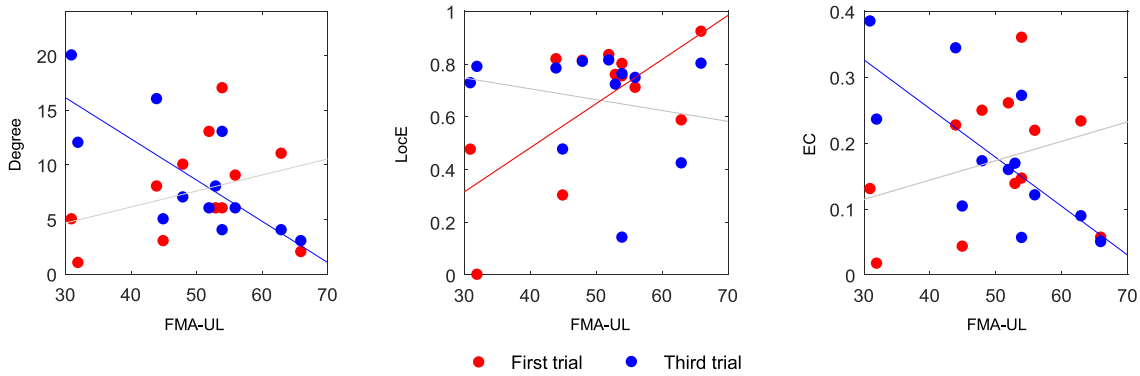

Fig. 6. Correlation with local properties based on the wPLI at Fz in the mu band. There are degree, local efficiency (LocE), and eigenvector centrality (EC) in the local properties. The red and blue dots indicate the local properties in the first and third trials, respectively. In specific, each dot means averaged local properties of the corresponding trial in all blocks on each subject. The solid lines represent linear fits to the data. The gray line refers to no significant correlations with a p-value of 0.05 or less, and the red or blue line indicates that each local property is statistically correlated with the FMA-UL.

V. Discussion

This study investigated the differences in the wPLI and DTF between healthy controls and chronic stroke patients during motor imagery. In motor networks including the DLPFC, there was no difference in the wPLI between the two groups. However, the DTF in stroke patients was significantly higher than in healthy controls. Moreover, the differences in network properties between consecutive trials were explored within each group. According to consecutive trials in healthy controls, there was no difference in the network properties, but a decrease in the network properties was observed in stroke patients. Based on these findings, the wPLI, DTF, and their network properties were significantly correlated with the FMA-UL in stroke patients. In addition, we predicted the FMA-UL in stroke patients using correlated connectivity measures and network properties.

A. Differences in Interregional Interactions Over Time

We found that the local properties decreased in stroke patients from the first to the third trial during consecutive motor imagery. During motor imagery, a decrease in degree, local efficiency, and eigenvector centrality was found over node F3 (left DLPFC) in the stroke patients. However, no changes were observed in the healthy controls. This finding can be explained from the perspective of motor imagery learning [15]. In healthy controls, previous imaginations do not affect them. However, in stroke patients, the impact of the first trial affects later trials in terms of motor learning. Specifically, the oscillatory activity over the ipsilesional hemisphere of stroke patients tends to decrease through repeated trials during motor imagery [15]. This phenomenon is thought to affect brain connectivity.

The role of the DLPFC is motor planning, including in preparatory motor networks [49], which occurs in the early phases of motor training [50]. In addition, the network properties in the DLPFC are associated more with higher-order cognitive motor preprocessing through motor control [51]. Similar to the SMA, it also appears to play a role in movement inhibition [49]. In this sense, because the motor network of stroke patients was basically broken, the activity of the local network over the left DLPFC was considered to be stronger in the early stages than in healthy controls.

It is also noteworthy that the local properties during consecutive motor imagery in stroke patients and healthy controls differ more than the global property. Mazrooyisebdani *et al.* [52] reported that an alteration in regional centrality could be used to evaluate the motor network. In stroke patients, in particular, only a part of the brain is damaged, and thus the local network seems to show a difference in brain connectivity in consideration of neural plasticity. There were no differences in the global network under a longitudinal change before or after the rehabilitation of stroke patients, although significant differences were observed in the local network.

It is necessary to ensure that changes in connectivity with motor imagery trials do not affect other factors such as fatigue, focused attention effects, or understanding of the task. First of all, the motor imagery task was performed, so we focused on the mu and beta bands and motor networks (brain central regions) related to movement. On the other hand, fatigue is connected with increased frontal theta and parietal alpha activities [53]. In addition, attention is associated with parieto-occipital alpha amplitude [54]. In this respect, it is believed that our findings would not be the effect of fatigue and attention. Regarding the understanding of the task, the understanding from the first to third trials would not have improved because they had already gone through sufficient explanation and practice before starting the task. Above all, the interval between each trial is 1.3 sec. Therefore, factors such as fatigue, attention, or understanding of the task do not seem likely to affect the brain in just 1.3 sec, and our findings are believed to be related to performing motor imagery tasks.

B. Comparisons Between wPLI and DTF

There was no difference in the wPLI, but there was a clear difference in the DTF for motor networks in both groups. Functional connectivity, such as the wPLI, indicates the patterns

Authorized licensed use limited to: Korea University. Downloaded on July 20,2022 at 03:25:32 UTC from IEEE Xplore. Restrictions apply.

of cross-correlations between two signals expected from these brain dynamics, whereas effective connectivity such as DTF indicates patterns of causal relationships between two signals as directed information flow [20]. Oscillations in EEG signals are an important feature of neurophysiological dynamics, which are thought to restrict and supervise neural activity within and between brain networks across a wide range of temporal and spatial information [55]. The causal connectivity of motor-related core regions was also observed during motor imagery using functional magnetic resonance imaging (fMRI), which has a high spatial resolution [56]. In this regard, the directional connectivity of the motor network is considered to be a clear representation of the motor functions evaluated by the FMA-UL in stroke patients.

The DTF in stroke patients was significantly higher than that in healthy controls in the motor network. In particular, these features were prominently represented in the DTF from the SMA. The SMA plays a prominent role in supporting limited motor outcomes. In other words, this region is directly related to descending motor control. In particular, the mu band serves as a medium for allocating computational resources, which is thought to be directly connected to motor planning from the perspective of motor learning [15]. In addition, the SMA suppresses the M1 during motor imagery. This means that the SMA sends signals to the M1 to prevent motor execution [57]. It is believed that the effect of SMA on M1 is different in motor imagery and motor execution. Although the effect of SMA is constant because even stroke patients actually move during motor execution, the suppression influences of SMA may vary from patient to patient because they do not actually move during motor imagery [58]. In this respect, motor imagery may provide more insights into brain connectivity than motor execution [59].

The high DTF of stroke patients in the SMA indicates that the patient's motor network is damaged, so stronger signals are needed to both actually move and imagine movement compared to healthy controls. In this regard, DTF over the SMA could be highly associated with motor impairments. The performance of motor imagery increased as the activity of the bilateral SMA in the stroke patients improved [8]. In other words, the SMA plays a direct role in motor imagery concerning the motor intention network. Therefore, it is possible to observe higher DTF from the SMA in stroke patients than in healthy controls. Meanwhile, in stroke patients, higher DTF from SMA was directed to the contralesional motor cortex. Other studies have also found that brain connectivity increased after stroke, which is related to compensating the motor function of the affected hand [60].

Taken together, a stronger DTF is a sign of motor network damage. In patients with mild traumatic brain injury, the local area of the damaged brain was rather weakened in connectivity, but the long-distance connection was rather stronger [61]. This is believed to be associated with neural plasticity, and in the end, similar characteristics will occur in the damaged brain of stroke patients.

The motor network also had different characteristics in each band between the two groups. In fact, in the mu band, the DTF from Cz to C3 was statistically higher in the stroke patient than in healthy controls. However, this was not found in the beta band. The mu band activity focuses on the oscillatory activity before the stimulus, whereas the beta band is activated during kinetic motor imagery learning [15]. Therefore, the network differences between stroke patients and healthy controls over both the mu and beta bands are not the same.

C. Relationship With Motor Score Using Connectivity

Interestingly, DTF from node C4 and to node C4 in stroke patients was related to FMA-UL in the mu and beta bands, respectively. In chronic stroke patients, it is known that contralesional M1 is constructed by an inefficient network owing to damage in the brain regions [1]. To compensate for this, the contralesional M1 is formed by a powerful sub-network after stroke and is observed in chronic stroke patients. In other words, stroke patients with motor impairments had more activated motor networks, specifically the contralateral M1, left DLPFC, and PMA. The motor imagery decreases contralesional compensation in stroke patients [62]. In this respect, the severe motor impairments lead to a relatively small amount of compensation reduction, resulting in a high mu DTF from the contralesional motor cortex. This phenomenon is consistent with the fact that network properties are higher in stroke patients than in healthy controls. Similarly, stroke patients require more activity in motor planning, which is clearly correlated with motor function.

Regarding network properties, we mainly observed a correlation between the local properties over node Fz and FMA-UL in stroke patients. PMA is considered to be included in the compromised sub-network after stroke. Therefore, in previous studies, the coupling strength from the PMA to the SMA during motor imagery was higher than that during motor execution in healthy subjects [10]. The PMA is also associated with internal modeling and motor planning during motor imagery in healthy subjects as shown by fMRI studies [63]. Likewise, stroke patients with motor disabilities require more active motor planning.

The reason why other regions related to motor planning is more prominent than the M1 is because of our novel paradigm. Our paradigm can actually observe that subjects performed their motor imagination correctly. Previous studies reported differences between correct and incorrect trials during motor imagery [10]. Clear differences could be seen in repeated finger tapping because we used only correct trials during motor imagery.

D. Evaluation of Regression Model Using Network Properties

Compared with functional connectivity alone, the predictive performance using the PLI was higher than that using coherence, GMA-based local efficiency, and the wPLI. However, the performance using DTF for representing the causality between two nodes was outperformed compared to using functional connectivity such as the PLI and wPLI. Characterizing brain networks in terms of functional specialization can only provide a limited explanation of the neurological basis of the intrinsic process [64]. Furthermore, directed connectivity indicates specific information to determine how and if brain activity in the PMA and SMA influences activity in the M1 during motor

Authorized licensed use limited to: Korea University. Downloaded on July 20,2022 at 03:25:32 UTC from IEEE Xplore. Restrictions apply.

imagery [57]. In this respect, causal indicators represent the highest performance in the connectivity measures.

Based on this relationship with the network properties, we achieved an FMA-UL prediction with high accuracy in stroke patients. Many studies suggest that network properties based on connectivity measures can better explain the brain [18]. Network properties are considered to be the best predictor of brain reorganization because they describe global and local brain networks based on mathematical models, beyond merely explaining the relationship between two nodes [20]. Furthermore, compared to previous studies using resting-state data or motor execution data, higher performance was achieved due to the direct use of brain connectivity during motor imagery when the motor network was activated. Taken together, our results are believed to enable better prediction with brain connectivity during motor imagery because motor imagery performance may vary depending on the severity of motor impairments.

E. Limitation

This study had several limitations. First, the sample size of stroke patients was small. In the future, this study should be conducted with more patients in a cohort study and with other patients with motor dysfunction. Second, electromyography signals were not measured to check muscle movement during motor imagery. However, our paradigm can investigate whether the subjects actually conducted motor imagery. More precisely, the trials that the motor imagery was not clearly performed could be excluded. In this regard, our paradigm might have been more effective than electromyography measurements in that EEG signals with incorrect and correct responses during motor imagery are different [10]. Third, the characteristics of the lesions in stroke patients, such as the location, type of stroke, and size were not considered. Therefore, further research based on these characteristics is required. Next, healthy controls used only their dominant hand when performing the motor imagery finger tapping task. Thus, this study failed to directly explore the small difference that occurs from non-dominant hands directly. It would be beneficial to directly compare the differences between dominant and non-dominant hands during motor imagery in the future. In addition, matching the side of stroke patients with those recorded with dominant and non-dominant in healthy controls may be a new suggestion to explore novel findings. Therefore, research related to this would also be investigated. Finally, sensor-level connectivity may not be reliable because of the volume conduction effect. Nevertheless, the connectivity estimators we used, the wPLI and DTF, are designed to be robust to this effect [16], and access from source-space is still required.

VI. Conclusion

We presented the brain connectivity and network properties during consecutive motor imagery as decoded from EEG signals compared to healthy controls. In addition, motor impairments based on the FMA-UL in stroke patients were predicted using connectivity measures and network properties. We demonstrated that the proposed approach using network properties is superior to conventional predictors. The higher performance using causal connectivity compared to functional connectivity and better prediction using network properties than connectivity measures provided insights about the brain network to explain brain reorganization after stroke. The proposed predictor can be used to predict motor recovery and motor function in stroke patients by revealing that network properties are associated with motor impairments. It could be vital in establishing more effective rehabilitation strategies in that motor imagery training itself helps in the rehabilitation of motor functions. Therefore, our findings could help enhance rehabilitation strategies according to motor impairments using the predicted FMA-UL based on the network properties.

References

[1] J. M. Antelis *et al.*, "Decoding upper limb movement attempt from EEG measurements of the contralesional motor cortex in chronic stroke patients," *IEEE Trans. Biomed. Eng.*, vol. 64, no. 1, pp. 99–111, Jan. 2017.

[2] N. Cheng *et al.*, "Brain-computer interface-based soft robotic glove rehabilitation for stroke," *IEEE Trans. Biomed. Eng.*, vol. 67, no. 12, pp. 3339–3351, Dec. 2020.

[3] R. Foong *et al.*, "Assessment of the efficacy of EEG-based MI-BCI with visual feedback and EEG correlates of mental fatigue for upper-limb stroke rehabilitation," *IEEE Trans. Biomed. Eng.*, vol. 67, no. 3, pp. 786–795, Mar. 2020.

[4] A. R. Fugl-Meyer *et al.*, "The post-stroke hemiplegic patient. 1. a method for evaluation of physical performance," *Scand. J Rehabil. Med.*, vol. 7, no. 1, pp. 13–31, 1975.

[5] N. Riahi, V. A. Vakorin, and C. Menon, "Estimating fugl-meyer upper extremity motor score from functional-connectivity measures," *IEEE Trans. Neural Syst. Rehabil. Eng.*, vol. 28, no. 4, pp. 860–868, Apr. 2020.

[6] J. Mladenovic *et al.*, "Towards identifying optimal biased feedback for various user states and traits in motor imagery BCI," *IEEE Trans. Biomed. Eng.*, vol. 69, no. 3, pp. 1101–1110, Mar. 2022.

[7] M. Lee *et al.*, "Decoding finger tapping with the affected hand in chronic stroke patients during motor imagery and execution," *IEEE Trans. Neural Syst. Rehabil. Eng.*, vol. 29, pp. 1099–1109, 2021.

[8] C.-H. Park *et al.*, "Which motor cortical region best predicts imagined movement?," *Neuroimage*, vol. 113, pp. 101–110, 2015.

[9] N. Mizuguchi *et al.*, "Brain activity during motor imagery of an action with an object: A functional magnetic resonance imaging study," *Neurosci. Res.*, vol. 76, no. 3, pp. 150–155, 2013.

[10] Y. K. Kim *et al.*, "Changes in network connectivity during motor imagery and execution," *PLoS One*, vol. 13, no. 1, 2018, Art. no. e0190715.

[11] A. Spiegler, B. Graimann, and G. Pfurtscheller, "Phase coupling between different motor areas during tongue-movement imagery," *Neurosci. Lett.*, vol. 369, no. 1, pp. 50–54, 2004.

[12] M. Lee, J.-G. Yoon, and S.-W. Lee, "Predicting motor imagery performance from resting-state EEG using dynamic causal modeling," *Front. Hum. Neurosci.*, vol. 14, 2020, Art. no. 321.

[13] F. D. V. Fallani *et al.*, "Multiscale topological properties of functional brain networks during motor imagery after stroke," *Neuroimage*, vol. 83, pp. 438–449, 2013.

[14] C. Calautti *et al.*, "The neural substrates of impaired finger tapping regularity after stroke," *Neuroimage*, vol. 50, no. 1, pp. 1–6, 2010.

[15] M. Lee *et al.*, "Motor imagery learning across a sequence of trials in stroke patients," *Restor. Neurol. Neurosci.*, vol. 34, no. 4, pp. 635–645, 2016.

[16] M. Vinck *et al.*, "An improved index of phase-synchronization for electrophysiological data in the presence of volume-conduction, noise and sample-size bias," *Neuroimage*, vol. 55, no. 4, pp. 1548–1565, 2011.

[17] C. J. Stam, G. Nolte, and A. Daffertshofer, "Phase lag index: Assessment of functional connectivity from multi channel EEG and MEG with diminished bias from common sources," *Hum. Brain Mapp.*, vol. 28, no. 11, pp. 1178–1193, 2007.

[18] M. Lee *et al.*, "Causal connectivity according to conscious experience in non-rapid eye movement sleep," in *Proc. IEEE Int. Conf. Syst., Man Cybern.*, 2019, pp. 2133–2138.

[19] S. Cekic, D. Grandjean, and O. Renaud, "Time, frequency, and time-varying granger-causality measures in neuroscience," *Statist. Med.*, vol. 37, no. 11, pp. 1910–1931, 2018.

Authorized licensed use limited to: Korea University. Downloaded on July 20,2022 at 03:25:32 UTC from IEEE Xplore. Restrictions apply.

[20] M. Rubinov and O. Sporns, "Complex network measures of brain connectivity: Uses and interpretations," *Neuroimage*, vol. 52, no. 3, pp. 1059–1069, 2010.

[21] J. I. Doerrfuss *et al.*, "Quantitative and qualitative EEG as a prediction tool for outcome and complications in acute stroke patients," *Clin. EEG Neurosci.*, vol. 51, no. 2, pp. 121–129, 2020.

[22] S. P. Finnigan *et al.*, "Quantitative EEG indices of sub-acute ischaemic stroke correlate with clinical outcomes," *Clin. Neurophysiol.*, vol. 118, no. 11, pp. 2525–2532, 2007.

[23] R. V. Sheorajpanday *et al.*, "Quantitative EEG in ischemic stroke: Correlation with functional status after 6 months," *Clin. Neurophysiol.*, vol. 122, no. 5, pp. 874–883, 2011.

[24] A. M. Chiarelli *et al.*, "Electroencephalography-derived prognosis of functional recovery in acute stroke through machine learning approaches," *Int. J. Neural Syst.*, vol. 30, no. 12, 2020, Art. no. 2050067.

[25] R. Mane *et al.*, "Prognostic and monitory EEG-biomarkers for BCI upper-limb stroke rehabilitation," *IEEE Trans. Neural Syst. Rehabil. Eng.*, vol. 27, no. 8, pp. 1654–1664, Aug. 2019.

[26] P. Trujillo *et al.*, "Quantitative EEG for predicting upper limb motor recovery in chronic stroke robot-assisted rehabilitation," *IEEE Trans. Neural Syst. Rehabil. Eng.*, vol. 25, no. 7, pp. 1058–1067, Jul. 2017.

[27] P. Tewarie *et al.*, "Relationships between neuronal oscillatory amplitude and dynamic functional connectivity," *Cereb. Cortex*, vol. 29, no. 6, pp. 2668–2681, 2019.

[28] B. Hordacre *et al.*, "Resting state functional connectivity measures correlate with the response to anodal transcranial direct current stimulation," *Eur. J. Neurosci.*, vol. 45, no. 6, pp. 837–845, 2017.

[29] D. Rathee *et al.*, "Brain-machine interface-driven post-stroke upper-limb functional recovery correlates with beta-band mediated cortical networks," *IEEE Trans. Neural Syst. Rehabil. Eng.*, vol. 27, no. 5, pp. 1020–1031, May 2019.

[30] G. R. Philips, J. J. Daly, and J. C. Príncipe, "Topographical measures of functional connectivity as biomarkers for post-stroke motor recovery," *J. Neuroeng. Rehabil.*, vol. 14, no. 1, pp. 1–16, 2017.

[31] C. M. Stinear *et al.*, "Lateralization of motor imagery following stroke," *Clin. Neurophysiol.*, vol. 118, no. 8, pp. 1794–1801, 2007.

[32] R. C. Oldfield *et al.*, "The assessment and analysis of handedness: The edinburgh inventory," *Neuropsychologia*, vol. 9, no. 1, pp. 97–113, 1971.

[33] A. Delorme and S. Makeig, "EEGLAB: An open source toolbox for analysis of single-trial EEG dynamics including independent component analysis," *J. Neurosci. Methods*, vol. 134, no. 1, pp. 9–21, 2004.

[34] M. Lee *et al.*, "Connectivity differences between consciousness and unconsciousness in non-rapid eye movement sleep: A TMS-EEG study," *Sci. Rep.*, vol. 9, no. 1, pp. 1–9, 2019.

[35] G. Niso *et al.*, "HERMES: Towards an integrated toolbox to characterize functional and effective brain connectivity," *Neuroinformatics*, vol. 11, no. 4, pp. 405–434, 2013.

[36] G. Plomp *et al.*, "The physiological plausibility of time-varying granger-causal modeling: Normalization and weighting by spectral power," *Neuroimage*, vol. 97, pp. 206–216, 2014.

[37] M. Drakesmith *et al.*, "Overcoming the effects of false positives and threshold bias in graph theoretical analyses of neuroimaging data," *Neuroimage*, vol. 118, pp. 313–333, 2015.

[38] F. de Vico Fallani *et al.*, "Structural organization of functional networks from EEG signals during motor learning tasks," *Int. J. Bifurcation Chaos*, vol. 20, no. 3, pp. 905–912, 2010.

[39] C.-L. Hung, C.-W. Chang, and T.-M. Hung, "Comparison of best and worst performance on EEG coherence in skilled dart players," *Psychophosiol.*, vol. 46, pp. 135–135, 2009.

[40] A. R. Anwar *et al.*, "Effective connectivity of cortical sensorimotor networks during finger movement tasks: A simultaneous fNIRS, fMRI, EEG study," *Brain Topogr.*, vol. 29, no. 5, pp. 645–660, 2016.

[41] S. Achard and E. Bullmore, "Efficiency and cost of economical brain functional networks," *PLoS Comput. Biol.*, vol. 3, no. 2, 2007, Art. no. e17.

[42] K. Alaerts *et al.*, "Functional organization of the action observation network in autism: A graph theory approach," *PLoS One*, vol. 10, no. 8, 2015, Art. no. e0137020.

[43] K. E. Joyce *et al.*, "A new measure of centrality for brain networks," *PLoS One*, vol. 5, no. 8, 2010, Art. no. e12200.

[44] X. Lei *et al.*, "Multimodal functional network connectivity: An EEG-fMRI fusion in network space," *PLoS One*, vol. 6, no. 9, 2011, Art. no. e24642.

[45] A. R. McIntosh and N. J. Lobaugh, "Partial least squares analysis of neuroimaging data: Applications and advances," *Neuroimage*, vol. 23, pp. S250–S263, 2004.

[46] J. Wu *et al.*, "Connectivity measures are robust biomarkers of cortical function and plasticity after stroke," *Brain*, vol. 138, no. 8, pp. 2359–2369, 2015.

[47] R. Varatharajan, G. Manogaran, and M. Priyan, "A Big Data classification approach using LDA with an enhanced SVM method for ECG signals in cloud computing," Multimed. *Tools Appl.*, vol. 77, no. 8, pp. 10195–10215, 2018.

[48] F. Pesarin and L. Salmaso, "The permutation testing approach: A review," *Statistica*, vol. 70, no. 4, pp. 481–509, 2010.

[49] R. M. Hardwick *et al.*, "Neural correlates of action: Comparing meta-analyses of imagery, observation, and execution," *Neurosci. Biobehav. Rev.*, vol. 94, pp. 31–44, 2018.

[50] A. Pascual-Leone *et al.*, "The role of the dorsolateral prefrontal cortex in implicit procedural learning," *Exp. Brain Res.*, vol. 107, no. 3, pp. 479–485, 1996.

[51] T. Hanakawa, M. A. Dimyan, and M. Hallett, "Motor planning, imagery, and execution in the distributed motor network: A time-course study with functional MRI," *Cereb. Cortex*, vol. 18, no. 12, pp. 2775–2788, 2008.

[52] M. Mazrooyisebdani *et al.*, "Evaluation of changes in the motor network following BCI therapy based on graph theory analysis," *Front. Neurosci.*, vol. 12, 2018, Art. no. 861.

[53] L. J. Trejo *et al.*, "EEG-based estimation and classification of mental fatigue," *Psychology*, vol. 6, no. 05, 2015, Art. no. 572.

[54] P. Sauseng *et al.*, "A shift of visual spatial attention is selectively associated with human EEG alpha activity," *Eur. J. Neurosci.*, vol. 22, no. 11, pp. 2917–2926, 2005.

[55] P. A. Stokes and P. L. Purdon, "A study of problems encountered in granger causality analysis from a neuroscience perspective," *Proc. Natl. Acad. Sci. U. S. A.*, vol. 114, no. 34, pp. E7063–E7072, 2017.

[56] S. Hu *et al.*, "Comparison analysis: Granger causality and new causality and their applications to motor imagery," *IEEE Trans. Neural. Netw. Learn. Syst.*, vol. 27, no. 7, pp. 1429–1444, Jul. 2016.

[57] C. H. Kasess *et al.*, "The suppressive influence of SMA on M1 in motor imagery revealed by fMRI and dynamic causal modeling," *Neuroimage*, vol. 40, no. 2, pp. 828–837, 2008.

[58] S. Bajaj *et al.*, "Brain effective connectivity during motor-imagery and execution following stroke and rehabilitation," *NeuroImage Clin.*, vol. 8, pp. 572–582, 2015.

[59] T. Cattai *et al.*, "Phase/amplitude synchronization of brain signals during motor imagery BCI tasks," *IEEE Trans. Neural Syst. Rehabil. Eng.*, vol. 29, pp. 1168–1177, 2021.

[60] Y. Zhang *et al.*, "Relationship between functional connectivity and motor function assessment in stroke patients with hemiplegia: A resting-state functional MRI study," *Neuroradiol.*, vol. 58, no. 5, pp. 503–511, 2016.

[61] S. I. Dimitriadis *et al.*, "Functional connectivity changes detected with magnetoencephalography after mild traumatic brain injury," *NeuroImage Clin.*, vol. 9, pp. 519–531, 2015.

[62] X. Xiong *et al.*, "Motor imagery training reduces contralesional compensation in stroke patients with moderate to severe upper limb impairment," in *Proc. 10th Int. IEEE/EMBS Conf. Neural Eng.*, 2021, pp. 876–879.

[63] A. Zabicki *et al.*, "Subjective vividness of motor imagery has a neural signature in human premotor and parietal cortex," *Neuroimage*, vol. 197, pp. 273–283, 2019.

[64] L. Astolfi *et al.*, "Estimation of the cortical connectivity by high-resolution EEG and structural equation modeling: Simulations and application to finger tapping data," *IEEE Trans. Biomed. Eng.*, vol. 52, no. 5, pp. 757–768, May 2005.

Authorized licensed use limited to: Korea University. Downloaded on July 20,2022 at 03:25:32 UTC from IEEE Xplore. Restrictions apply.